

Future global water scarcity partially moderated by vegetation responses to atmospheric CO₂ and climate change

Jessica Stacey^{1,2}, Richard A. Betts^{1,2}, Andrew Hartley², Lina Mercado^{3,4}, Nicola Gedney²

¹Global Systems Institute, University of Exeter, Exeter, EX4 4QJ, UK

5 ²Met Office Hadley Centre, Exeter, EX1 3PB, UK

³Environment, Science & Economy, University of Exeter, Exeter, EX4 4QJ, UK

⁴UK Centre for Ecology and Hydrology, Wallingford, EX10 8BB, UK

Correspondence to: Jessica Stacey (jessica.stacey@metoffice.gov.uk)

Abstract. Accurate water scarcity projections are essential for effective adaptation strategies. Most existing studies rely on hydrology models that often neglect the effects of plant physiological responses to rising CO₂ on the water cycle, such as reduced stomatal opening, which can decrease transpiration and enhance water availability over large scales. To evaluate how physiological and structural plant responses to rising CO₂ and subsequent climate change affect water scarcity in typical impact studies, we replicate their experimental design by driving an offline land surface model with Earth system model output. Under a high-emission climate scenario, our simulations suggest that the combined effects of these plant responses partially alleviate the Water Scarcity Index (WSI) for most regions, largely due to CO₂-induced stomatal closure, although CO₂- and climate-induced vegetation changes do exacerbate water scarcity in some places, particularly arid regions. For the period 2076–2095, incorporating all plant responses to CO₂ and climate change reduces global median WSI by approximately 12%. Furthermore, across 291 river basins, 138 basins show lower median WSI (by 10-70%), representing 80% of the global population, while 11 basins show higher WSI (by 10-60%), representing 0.2% of the population. These model results highlight the potential for plant responses to CO₂ to somewhat moderate water scarcity, noting water scarcity is still projected to worsen in many regions, including highly populated areas. There is an urgent need to gather empirical evidence on the strength of plant responses to CO₂ at large scales to address modelling uncertainties.

Short summary. Plants typically transpire less with rising atmospheric carbon dioxide, leaving more water in the ground for human use, but many future water scarcity assessments ignore this effect. We use a land surface model to examine how plant responses to carbon dioxide and climate change affect future water scarcity. Our results suggest that including these plant responses increases overall water availability for most people, highlighting the importance of their inclusion in future water scarcity studies.

1 Introduction

30 Throughout this manuscript, we use the following terminology:

- **Stomatal response** – changes in stomatal conductance (i.e., stomatal opening and closure)

- **Structural response** – changes in vegetation structure (leaf area and canopy coverage)
- **Physiological response (or forcing)** – CO₂-induced changes encompassing both stomatal behaviour and vegetation structure (leaf area and canopy coverage)

35

Water scarcity, where water demand exceeds available supply, is one of the greatest challenges of our time (FAO, 2017). Nearly half of the global population already faces severe water scarcity at some point each year, and as both population and consumption rates rise, water demand is escalating (Caretta et al. 2022). From 1992 to 2015, global freshwater resources per capita declined by over 25% (Ripple et al., 2017). Water availability, crucial for meeting this rising demand, depends on the balance between land precipitation and evapotranspiration, both of which are strongly affected by human activities, including climate change. Climate change is altering precipitation patterns and near-surface meteorological conditions, driving more frequent hydrological extremes and higher evaporative demand (Seneviratne et al., 2021). Human interventions—such as groundwater over-abstraction, dam construction, and water diversion—further disrupt water supply, while pollution threatens the availability of clean water. Accurately forecasting future water supply and demand remains a complex but vital task for informing long-term adaptation strategies (Caretta et al., 2022). Current impact studies on future water scarcity are typically based on output from hydrology models driven by climate model outputs (e.g., Dolan et al., 2021; Gosling and Arnell, 2016; Greve et al., 2018; Haddeland et al., 2014). While hydrology models are powerful tools for understanding, managing, and planning water resources, they often lack a representation of vegetation response to rising levels of CO₂ and climate change. In this study, we investigate the influence that vegetation responses to atmospheric CO₂ and climate change have on water scarcity projections.

50

Vegetation is crucial to the global water cycle and therefore to water availability for humans. Large-scale changes in vegetation type and coverage are already occurring due to climate change and human activities, such as deforestation. Vegetation plays a key role in precipitation generation, with approximately 60% of terrestrial precipitation originating from land via evapotranspiration – primarily through plant transpiration (Schneider et al., 2017; Wei et al., 2017). Vegetation also influences other hydrological processes, including infiltration, interception, and runoff (Caretta et al., 2022). Climate change continues to alter vegetation types and coverage globally, as regions experience more or less favourable conditions. Increased vegetation growth has been observed in many areas (Xu et al., 2017; Yu et al., 2018; Zhu et al., 2016), while droughts and heatwaves have heightened plant stress and mortality (Parmesan et al. 2022).

60

Rising atmospheric CO₂ concentrations also impact the water cycle by altering plant physiology. Plants continuously adjust the widths of their stomatal openings to maximise photosynthesis while minimising water loss (Cowan, 1978). Under higher atmospheric CO₂, plants typically reduce their stomatal openings, as they can maintain higher rates of photosynthesis at increased leaf-level water-use efficiency, thereby decreasing transpiration (Battipaglia et al., 2013; Field et al., 1995; Norby and Zak, 2011). As less water is lost through transpiration, more water remains in the soil and at the surface, contributing to

65

increased runoff and soil moisture levels (Fowler et al., 2019; Gedney et al., 2006). However, higher CO₂ generally enhances photosynthesis, known as the CO₂ fertilisation effect, leading to increased vegetation growth and thus overall canopy transpiration due to a higher number of stomata, even as individual stomatal openings are reduced (Betts et al., 1997). At the canopy-level, this effect can offset or even reverse the increase in runoff from reduced stomatal openings (Cowling and Field, 2003; Piao et al., 2007; Ukkola et al., 2016). The net effect on canopy transpiration thus depends on the balance between these two opposing factors, which varies greatly between different plant species and climatic biomes (Norby and Zak 2011).

Better understanding of vegetation-water-atmosphere interactions, in both historical observations and under future climate change scenarios (e.g., Betts et al., 2007; Gedney et al., 2006) has been made possible with the introduction of Land Surface Models (LSMs). LSMs simulate complex interactions between the atmosphere, land surface, and sub-surface, including energy and water fluxes, carbon cycling, and soil processes. Dynamic vegetation schemes in LSMs have been made increasingly realistic over the past few decades (Fisher and Koven, 2020). They typically simulate vegetation coverage, canopy height and leaf area index for a limited number of generalised plant functional types, driven by carbon fluxes and vegetation competition. Including dynamic vegetation in climate models is essential for capturing critical changes in land surface and plant physiology that influence the climate system and hydrological cycle. Yet, these schemes are still absent from many hydrology models.

Advances in LSMs have improved understanding of how plant physiological responses to rising CO₂, herein ‘physiological forcing’ (which, in this study also refers to changes in vegetation coverage and leaf area) impact the water cycle. An early study by Wigley and Jones (1985) was one of the first to link CO₂-driven changes in plant evapotranspiration (ET) to runoff. As land surface and climate models have advanced, effects of CO₂-induced vegetation growth on the water cycle have also been analysed alongside stomatal closure. Betts et al. (1997) projected that increased vegetation cover could partially offset the projected reduction in ET. Gedney et al. (2006) attributed rising historical continental river runoff records to CO₂-induced stomatal closure. However, Piao et al. (2007) suggested that physiological forcing *reduced* global runoff when CO₂-induced leaf area increases were also considered from 1901 to 1999. Subsequent modelling studies have also concluded that CO₂-induced stomatal closure and leaf area increases together generally *increase* projected global runoff in the current generation of models. For instance, doubling CO₂ in climate models led to global mean runoff increases of 6% (Betts et al., 2007) and 8-9% (Cao et al., 2010) relative to preindustrial; comparable to the impact of radiative forcing. Further studies have suggested that physiological responses to rising CO₂ affect the hydrological cycle differently around the globe, although generally suggest increased runoff, especially in the tropics (Davie et al., 2013; Fowler et al., 2019; Lemordant et al., 2018; Yang et al., 2019), reduced drought severity (Swann et al., 2016) and increased flood risk (Kooperman et al., 2018). Conversely, runoff reductions are suggested in more arid locations, including the mid-latitudes in model projections (Mankin et al., 2019) and parts of Australia in observations (Ukkola et al., 2016). Moreover, a recent study by Wei et al. (2024) suggested physiological forcing had limited effect on observed global streamflow. However, the consensus between most studies currently suggests that the

100 stomatal response to CO₂ has a dominant effect over the structural responses at the global scale, particularly in future climate projections.

105 Water scarcity is a complex and multifaceted issue influenced by water availability, demand, and quality. Many future water scarcity projections rely on standalone hydrology models driven by global climate model outputs (e.g., Dolan et al., 2021; Gosling and Arnell, 2016; Greve et al., 2018; Haddeland et al., 2014; Schewe et al., 2013). These studies have generally projected worsening water scarcity in many regions due to both climate change and rising demand, with the most affected areas including parts of northern and southern Africa, south and southeast Asia, Australia, parts of Europe, the Middle East and the western United States. However, these hydrology models often do not account for vegetation responses to atmospheric CO₂ and climate change.

110 Few studies have explored the influence of physiological forcing on water scarcity-related variables. Wiltshire et al. (2013a, b) suggested that when both climate change and CO₂ effects are considered, the number of people experiencing water stress decreases. Notably, Wiltshire et al. (2013a) projected that physiological forcing could reduce the population under high water stress by approximately 200 million by the end of the century, an impact comparable to that of climate change alone. However, while their water stress indicator accounted for population growth, it did not consider varying water demands due to different living standards. Wang and Sun (2023) also examined socioeconomic exposure to drought under various Shared Socioeconomic Pathways finding that physiological forcing could increase extreme drought frequency by around 2% in the 2030s, particularly in arid and semi-arid regions, but this influence shifted to a decrease by the 2050s. However, their study only used fully coupled models and did not replicate the experimental setup typically used in hydrology studies—such as driving standalone hydrology models with climate model outputs—and therefore did not directly address the impact of physiological forcing in hydrological studies.

125 Understanding the extent to which dynamic plant processes affect metrics like water scarcity remains a critical research gap for the climate and hydrology impacts community. This study is the first to address this by replicating the experimental design of typical hydrology impact studies, i.e., running a standalone hydrology model without dynamic vegetation driven by climate model output, while adjusting plant responses to rising CO₂ and climate change through a land surface model. This approach allows us to estimate how vegetation's physiological and structural responses affect global water scarcity projections.

2 Methodology

2.1 Experimental design

130 The setup of the experiment has been carefully designed to best replicate the process used in water-related impact studies, i.e., a hydrology model run standalone and driven by climate model output. Here we use the Joint UK Land Environment

135 Simulator (JULES; Best et al., 2011; Clark et al., 2011) as the offline impact model. JULES has been driven by the bias-adjusted (following Lange, 2019) Earth system climate model HadGEM2-ES (Hadley Centre Global Environment Model version 2; Jones et al., 2011) resampled to 0.5 x 0.5 degrees horizontal resolution as part of the bias correction. We use the historic simulation from 1861 to 2005 and the “future” period 2006 to 2100 using Representative Concentration Pathway (RCP) 6.0. The earth system configuration JULES-ES is used following the setup for the Inter-Sectoral Impact Model Intercomparison Project (ISIMIP; <https://www.isimip.org/>) version 2b; details of the setup can be found in Mathison et al. (2023).

140 JULES is a suitable model for this study as it includes both a global hydrological cycle and dynamic vegetation scheme (Cox, 2001), enabling isolation of different vegetation structural and physiological processes to investigate their influence on the hydrological cycle. For our experiments, we use a combination of fixing the following two components in JULES:

- (1) the **plant physiological response to rising CO₂** by fixing CO₂ in JULES to 277ppm (representing preindustrial levels following protocol of the TRENDY project; Sitch et al., 2024).
 - (2) **vegetation spatial and temporal structural changes**, including Leaf Area Index (LAI; the ratio of leaf to ground area), by fixing the dynamic vegetation scheme in JULES to that at the start of the simulation.
- 145

Using a combination of fixing CO₂ and dynamic vegetation in JULES gives four simulations, all driven by identical climate model output. Taking the difference between two different simulations enables us to investigate the influence of different plant responses. Table 1 outlines the name of the simulations and which vegetation responses they include. A more expansive table can be found in Table A1. Note the naming conventions used in this study for each simulation and isolated factor follow the generic format: <Forcing factor(s)>: <Responding factor(s)>. The following acronyms have been used: ‘CLIM’ represents climate changes, ‘CO₂’ represents the atmospheric CO₂ changes, ‘VEG’ represents vegetation cover and LAI responses and ‘STOM’ represents stomatal responses.

150

155 Simulation 1 (S1) CLIM: STOM includes climate-induced stomatal changes only and is closest to a typical hydrology study with fixed vegetation coverage/LAI and physiological forcing. Simulation 2 (S2) CLIM: STOM+VEG includes climate-induced stomatal and vegetation coverage/LAI responses. Simulation 3 (S3) CLIM+CO₂: STOM includes CO₂- and climate-induced stomatal responses. Simulation 4 (S4) CLIM+CO₂: STOM+VEG includes all CO₂- and climate-induced stomatal and vegetation coverage/LAI responses and is closest to fully coupled Earth System Model. Different “isolated factors” are combined by taking the differences between simulations. CLIM: VEG (S2 – S1) represents climate effects on vegetation coverage/LAI. CO₂: STOM (S3 – S1) represents CO₂ effects on stomata. CO₂: STOM+VEG (S4 – S2) represents CO₂ effects on stomata and vegetation coverage/LAI. CO₂: STOM & CLIM+CO₂: VEG (S4 – S1) represents CO₂ effects on stomata and climate plus CO₂ effects on vegetation coverage/LAI and indicates the differences between a typical offline hydrology study

160

and the fully coupled ESM. Relative differences, as displayed in Figs. 2, 4, 8 and 9, are calculated by dividing the difference
 165 by the initial value, following the formula: $\frac{b-a}{a}$. Note that we do not analyse the influence of climate change alone in this study.

Table 1: Details of dynamic processes included in each of the simulations and isolated factors.

Simulation	Name	Climate-induced stomatal changes	Climate-induced veg. changes	CO ₂ -induced stomatal changes	CO ₂ -induced veg. changes
S1	CLIM: STOM	✓			
S2	CLIM: STOM+VEG	✓	✓		
S3	CLIM+CO ₂ : STOM	✓		✓	
S4	CLIM+CO ₂ : STOM+VEG	✓	✓	✓	✓
S2 - S1	CLIM: VEG		✓		
S3 - S1	CO ₂ : STOM			✓	
S4 - S2	CO ₂ : STOM+VEG			✓	✓
S4 - S1	CO ₂ : STOM & CLIM+CO ₂ : VEG		✓	✓	✓

For all simulations, the atmospheric CO₂ and meteorological input variables such as radiation, temperature, precipitation and
 windspeed, are identical, since they come from the driving climate model HadGEM2-ES output, as would be the case for a
 typical hydrology study. Furthermore, all simulations use atmospheric CO₂ concentrations from the driving climate model
 170 (RCP 6.0), noting that, in the preindustrial CO₂ simulation, atmospheric CO₂ has been fixed in JULES only and not the driving
 climate input data. Note that anthropogenic disturbance of land is not included in any of the simulations, so vegetation can be
 affected by changes in climate and CO₂ only. Some of the meteorological inputs from HadGEM2-ES are shown in Fig. 1.

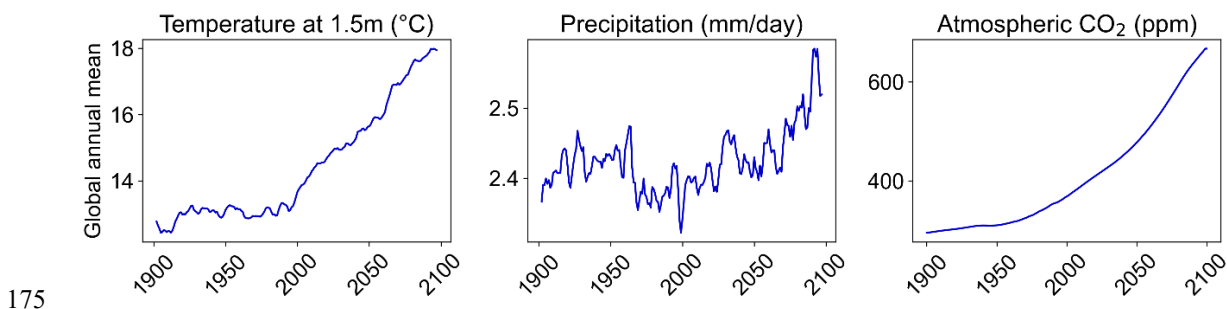
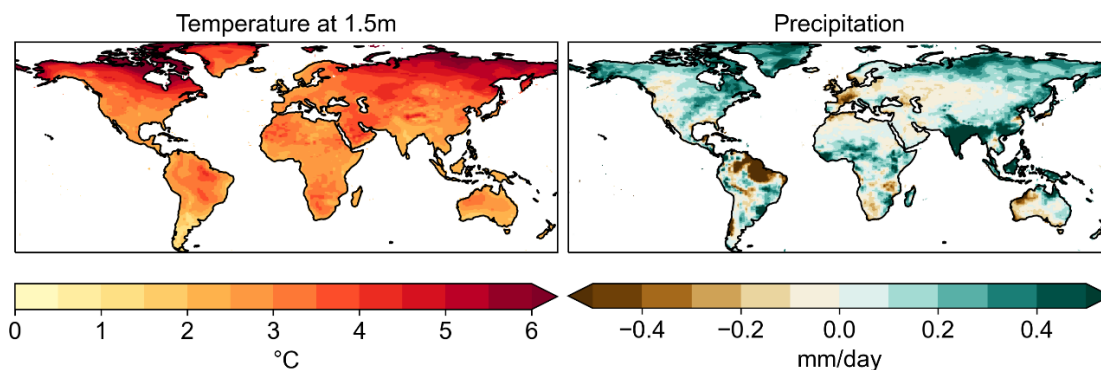


Figure 1a: Global annual mean timeseries for a) 1.5m temperature, b) precipitation and c) atmospheric CO₂ from driving climate model HadGEM2-ES used as input to JULES simulations (rolling 5-year mean for precipitation and temperature).



180 **Figure 1b: Mean changes from present (2006-2025) to future (2076-2095) for precipitation (left) and 1.5m temperature (right) from driving climate model HadGEM2-ES used as input to JULES simulations.**

Using the output from the four simulations in Table 1, we investigate the influence of physiological forcing and vegetation structural changes on global water scarcity. We calculate the Water Scarcity Index (WSI) to be the ratio of water demand to
 185 water supply (Falkenmark et al., 1989). The WSI is chosen as it is a simple and widely used indicator of water scarcity. We use a WSI of 0.2-0.4 to indicate mild or emerging water scarcity, and $WSI \geq 0.4$ for severe water scarcity, in line with Raskin and Gleick (1997) and Greve et al. (2018). Runoff is used as a proxy for water supply because it represents the fraction of precipitation that is not lost to evapotranspiration and is therefore available for water resources. Total runoff is taken from the output of the simulations and includes both surface (overland flow generated when precipitation exceeds
 190 infiltration capacity or soil saturation) and sub-surface runoff (lateral drainage through the soil column) at the grid box scale. Water demand has been downloaded from the ISIMIP database (<https://data.isimip.org/>), specifically ISIMIP2b from the global water sector (Gosling et al., 2023). The hydrology model used is H08 (Hanasaki et al., 2008a, b, 2018) driven by HadGEM2-ES, RCP 6.0 and shared socioeconomic pathway SSP2, which represents population and gross domestic product for the ‘middle of the road’ scenario (Riahi et al., 2017). Total water demand is represented by summing water withdrawal
 195 for irrigation (assuming unlimited water supply), domestic use and manufacturing.

Different approaches can be used to calculate the average WSI over space and time, which can considerably influence the results. Mostly, we have chosen to calculate WSI at the most granular spatial and temporal scale, which is monthly and by grid-box. The exception is when analysing by river basins in Figs. 8 and 9, where the sum of total supply and demand is
 200 computed for each basin before calculating WSI. The rationale is that, generally, all water within a river basin could ideally be used for all the population within that basin, noting in real life this is not always the case.

Since WSI is calculated as water demand divided by water supply, it can yield extremely high values where supply values are very low relative to demand. To moderate the impact of these extreme values, the *median* WSI is used for spatial and temporal

205 averaging in this study, as it provides a more robust measure less influenced by outliers. Additionally, median WSI is calculated
over larger spatial areas. Firstly, by the climate regions outlined in the Intergovernmental Panel on Climate Change (IPCC)
Sixth Assessment Report (AR6), consisting of 46 land regions based on a combination of geographic, climatic, and socio-
economic criteria (Fig. S2; Iturbide et al., 2020). Secondly, by Hydrosheds river basins
(<https://www.hydrosheds.org/products/hydrobasins>; Lehner and Grill, 2013).

210

Finally, population projections are for SSP2 from the ISIMIP2b data library (Piontek and Geiger, 2017), plotted in Fig. S1,
which are gridded at 0.5 x 0.5-degree resolution. These have been used to calculate projected population numbers by river
basin in Table 2 and Fig. 8.

2.2 The Joint UK Land Environment Simulator (JULES)

215 JULES is a process-based model simulating fluxes of carbon, water, energy and momentum between the land surface and
atmosphere. JULES is used as either an integral part of an Earth System Model such as UKESM1 (Sellar et al., 2019) or as
an independent land surface model driven by input data from observations or atmospheric models; in this study it is used in
the latter manner. Within JULES, the dynamic vegetation model predicts changes in leaf area and the fractional coverage of
13 different Plant Functional Types (PFTs; Harper et al., 2016) where each PFT is categorised by specific physiological
220 traits, and surface fluxes are calculated separately for each PFT. JULES uses a coupled canopy conductance and
photosynthesis model (Cox et al., 1998), based on Luening (1995), and TOPMODEL-type scheme to calculate soil moisture
and runoff; more details on both are in Appendix B.

3. Results

3.1 Vegetation and water cycle variables

225 The global-mean time series for water-cycle and vegetation variables (Fig. 2) reveal substantial divergence among simulations.
The largest relative differences are associated with the CO₂-induced stomatal response, as indicated by simulations including
CO₂: STOM, whose influence strengthens throughout the 21st century. In the climate-only simulation (S1), which reflects
typical hydrological modelling approaches, soil moisture declines over the century while transpiration increases slightly (Fig.
2d,i), likely driven by rising temperatures (Fig. 1a).

230

In contrast, when the CO₂-induced stomatal response is represented (S3 and S4), the projected soil-moisture decline is
substantially muted, coincident with ~20% reductions in both transpiration and stomatal conductance by 2100 (Fig. 2l,m).
Despite decreasing soil moisture, total runoff in S1 shows a modest increase in the latter half of the century (Fig. 2a). This
increase becomes ~10–12% larger when CO₂-induced stomatal closure is included (Fig. 2e).

235

CO₂-driven stomatal closure also dominates over the drying effect of CO₂-driven increases in leaf area. In CO₂: STOM+VEG, runoff continues to rise even with a ~30% increase in LAI (Fig. 2e,n). In contrast, climate-driven vegetation structural changes alone (CLIM: VEG) reduce LAI by ~20% (Fig. 2n), leading to a modest 3–5% reduction in transpiration (Fig. 2l) and only a slight enhancement in runoff (Fig. 2e).

240

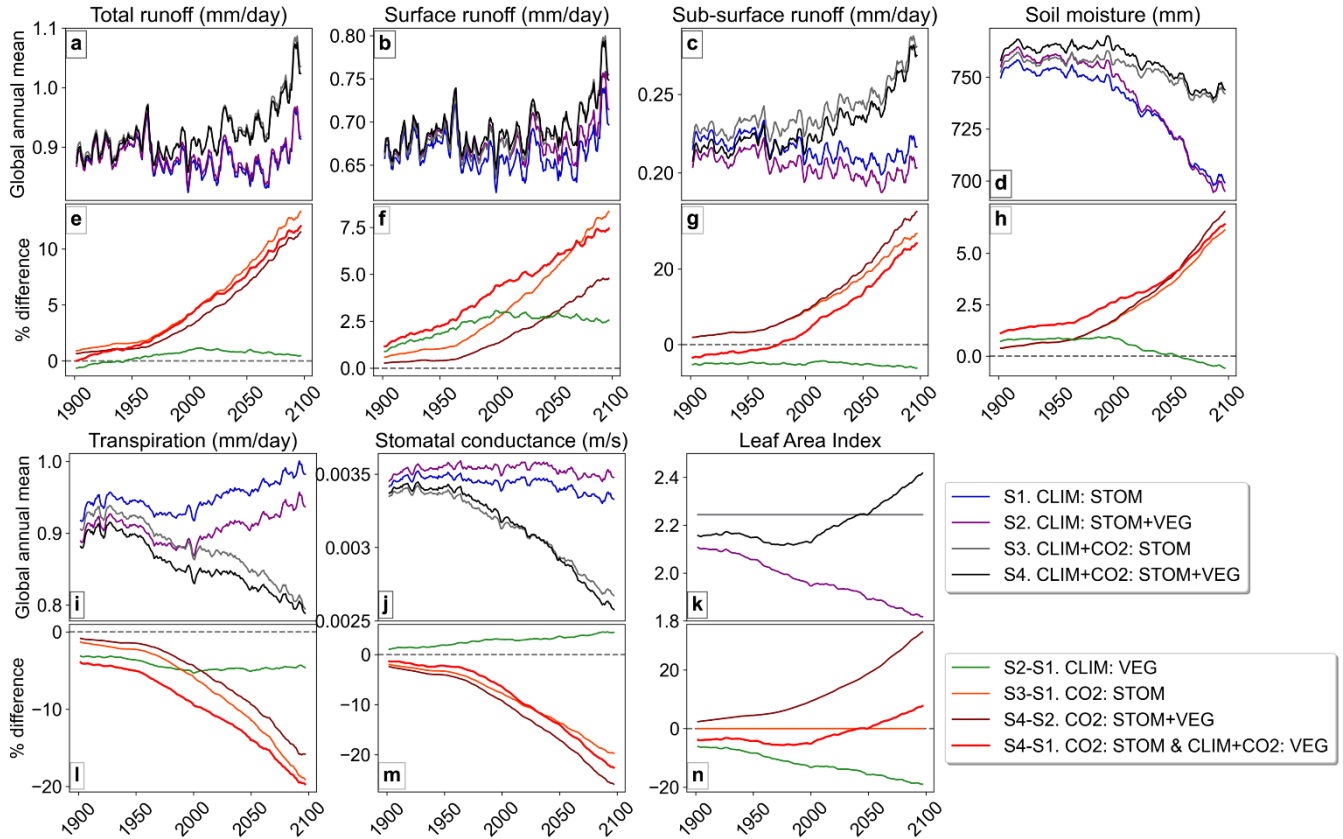


Figure 2: Global annual mean timeseries (rolling 5-year mean) in water cycle and vegetation variables in each simulation and the relative (%) difference between simulations.

245 While the CO₂-induced stomatal response contributes to overall surface wetting at the global scale (Fig. 2), its influence exhibits considerable spatial heterogeneity. Climate-driven runoff changes from the present (2006–2025) to the future (2076–2095) period are highly variable in both magnitude and direction (Fig. 3a) generally aligning with precipitation changes (Fig. 1b; right). When all vegetation and physiological changes are included in S4, the overall runoff and soil moisture pattern remain broadly similar to the climate-only simulation S1 (Fig. 3a,b,e,f) though increases are more evident in some regions, particularly the tropics, largely due to CO₂-induced stomatal closure. For instance, in CO₂: STOM+VEG, runoff increases are projected in many regions (Fig. 3i), especially the tropics and high northern latitudes, corresponding with transpiration

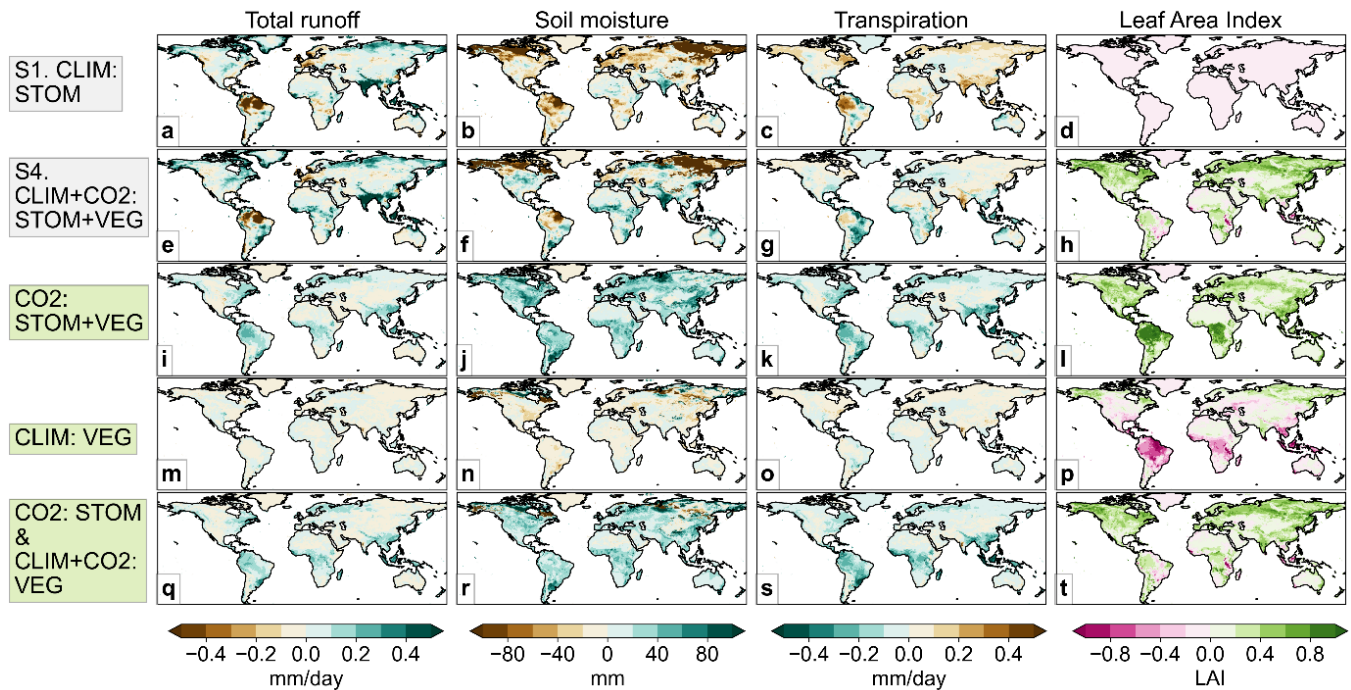
250

decreases (Fig. 3k). In areas with projected runoff decreases under climate forcing alone (Fig. 3a), such as in the Amazon, parts of the USA, northern and eastern Europe, the stomatal response mitigates drying and, in places such as central Africa, even *reverses* runoff decreases to increases (Fig. 3e).

255

In many regions, physiological forcing is driving runoff increases (Fig. 3i) despite CO₂-induced LAI increases (Fig. 3l), suggesting that stomatal closure outweighs the drying effect of enhanced leaf area. However, CO₂-induced LAI increases appear to drive slight runoff reductions across some areas, particularly in semi-arid and arid climates such as the Middle East and western USA (Fig. 3i,l). Although considerably smaller than the increases, these small runoff reductions could cause significant impacts in already water-stressed areas. In contrast, climate-driven vegetation structural changes (CLIM: VEG) have relatively limited impact on runoff, transpiration, and stomatal conductance, despite notable LAI changes in parts of the tropics and high latitudes (Fig. 3m-p).

260



265 **Figure 3: Global mean changes from present (2006-2025) to future (2076-2095) period in the climate-only simulation (top row), and the absolute difference when the various isolated factors are included.**

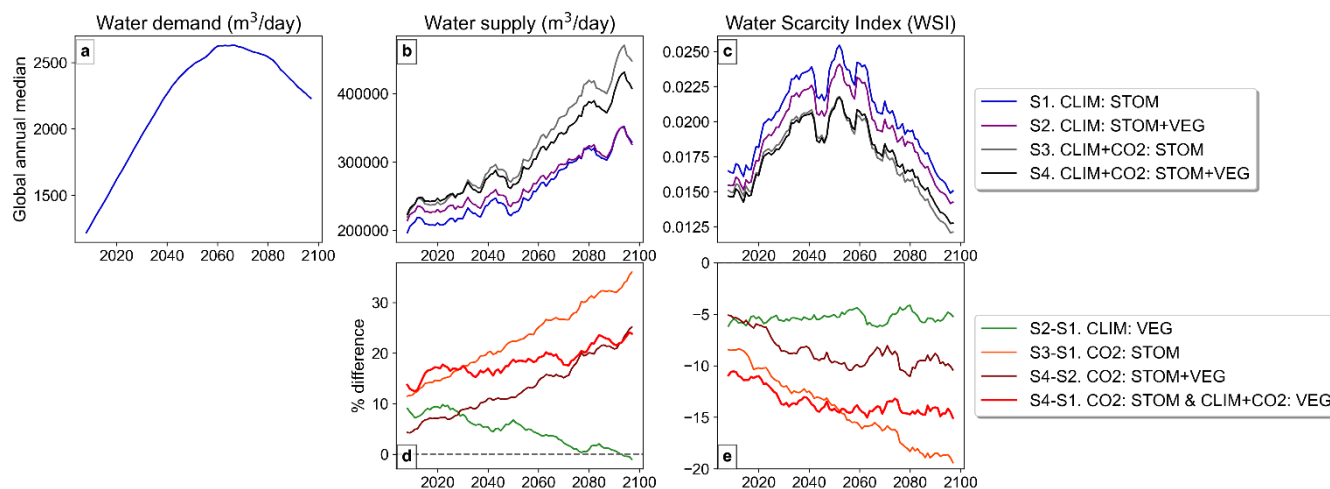
3.2 Water demand, supply and the Water Scarcity Index

Global median water demand, supply, and WSI are projected to increase over the coming decades under SSP2 and RCP 6.0 (Fig. 4a-c). However, while water demand and WSI peak and subsequently decline later in the century, JULES projects a

270 continued rise in global water supply, particularly in simulations S3 and S4 that include CO₂ effects on stomata (Fig. 4b).
 When the isolated effect of increased CO₂ on plant stomata is included (CO₂: STOM), global median water supply is
 approximately 30% higher by 2100; even when CO₂-induced structural changes are also included (CO₂: VEG+STOM), supply
 is around 20% higher by 2100. In contrast, the climate effects on vegetation have a comparatively small influence on global
 median water supply, and this influence diminishes further in the coming decades (Fig. 4d; CLIM: VEG).

275

These water supply increases correspond with consistent projected reductions in global median WSI throughout the century
 (Fig. 4c,e). The CO₂-induced stomatal response appears to ameliorate WSI by 15-20% toward the century-end shown by CO₂:
 STOM (Fig. 4e). However, when CO₂-induced LAI increases are also allowed in CO₂: STOM+VEG, the reduction in WSI is
 notably less at 8-10% in the second half of the century. Climate-induced vegetation changes also reduce global median WSI
 280 by around 5%, remaining consistent throughout the period. When all processes are included, the combined influence shown
 by S4 – S1 (Fig. 4e) results in a 10-15% reduction in WSI throughout the century.



285 **Figure 4: Annual global-median timeseries (rolling 5-year mean) of a) water demand, b) water supply, c) WSI in the four simulations and the % difference in d) supply and e) WSI due to the various isolated factors. Note, water demand is the same across all simulations.**

Under RCP 6.0 and SSP2, water demand for the present period is high in much of Europe, South and Southeast Asia and the
 USA (Fig. 5a). Water demand increases for most places, especially in the highly populated and developing regions of South
 290 Asia, as well as parts of Africa, but decreases are also seen for parts of Europe and China (Fig. 6a). Regions experiencing
 severe water scarcity (WSI \geq 0.4; Raskin, et al., 1997) in the present period (2006 - 2025), include most of India, the Middle
 East, eastern China and parts of South Africa, USA, and Europe (Fig. 5c). Large swathes of northern Africa are also
 experiencing severe water scarcity despite low demand (Fig. 5a). Even though global median WSI reduces later this century

in Fig. 4c, many of the already water scarce regions are projected to become even more water scarce by the future period
295 (2076-2095; Fig. 6c), as the demand grows, including in highly populated regions such as India.

The plots comparing the change in median WSI from the present (2006-2025) to the future (2076-2095) under scenarios with
and without plant processes (Fig. 6c,e) appear quite similar, suggesting that water demand and meteorological factors driving
water supply are the primary influences on WSI. Interestingly, the changes in supply between the S1 and S4 simulations (Fig.
300 6b,d) show greater difference than those for WSI, since the supply differences mainly occur in areas with low levels of water
scarcity, and therefore have less impact on WSI.

Despite the visual similarities between simulations with (Fig. 6e) and without (Fig. 6c) plant responses to CO₂ and climate,
the effect of plant responses on WSI is not negligible. The CO₂-induced stomatal response increases water supply in most
305 regions, especially in the tropics (Fig. 6f), resulting in corresponding reductions in WSI (Fig. 6g). When CO₂-induced
vegetation structural changes are also included in the CO₂: STOM+VEG simulations (Fig. 6h,i), overall supply still increases,
as the supply reductions associated with CO₂-driven structural vegetation expansion are relatively small and less apparent in
the plots. However, these modest reductions translate into substantial increases in WSI in arid regions such as the Middle East
and northern and southern Africa (Fig. 6i), where baseline water supply is already low. Climate-induced vegetation changes
310 shown in CLIM: VEG appear to have minimal impact on supply (Fig. 6j), yet there are substantial changes in WSI in some
areas, with increases in some places, including western India, although parts of southern and northern Africa show some
reductions (Fig. 6k). Finally, when all processes are combined in CO₂: STOM & CLIM+CO₂: VEG, supply predominantly
increases (Fig. 6l), even though WSI increases in many arid and semi-arid regions.

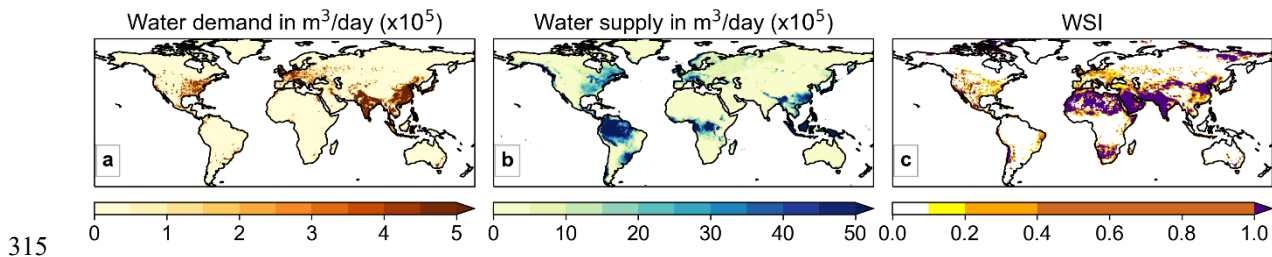
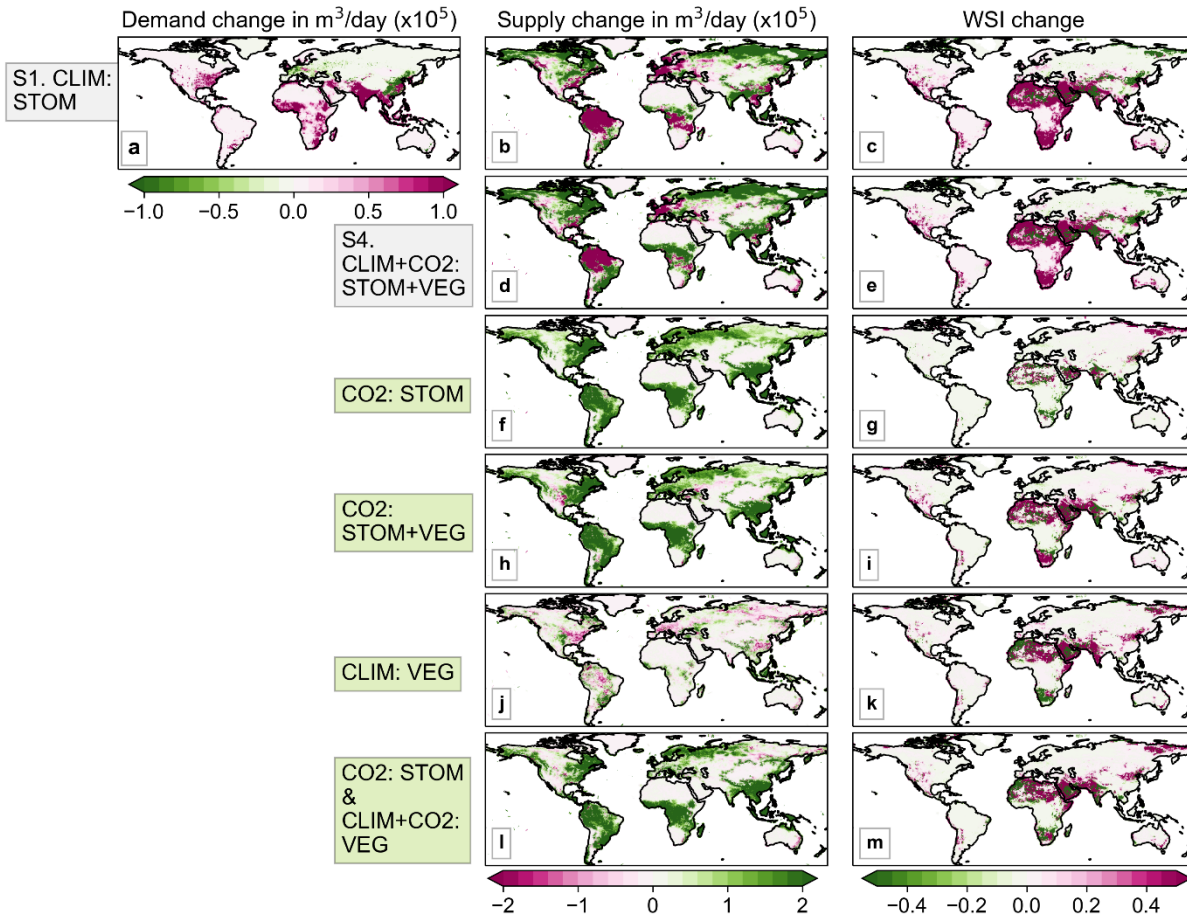


Figure 5: Median a) water demand, b) supply and c) Water Scarcity Index (WSI) for the period 2006-2025 in S1. CLIM: STOM.



320 **Figure 6: Median water demand, supply and Water Scarcity Index (WSI) change from the present (2006-2025) to future (2076-2095) period in simulations S1 and S4 (a-e), and the difference in supply and WSI when including the various isolated factors (f-m).**

The 25 IPCC AR6 climate regions with the highest monthly median WSI between 2076-2095 are shown in Fig. 7. The Arabian Peninsula region is projected to experience the highest median WSI, and South Asia is predicted to have the second highest (Fig. 7; left panel). Comparing with the 2006-2025 present period (Fig. S3), nearly all these regions are projected to increase in median WSI by the end of the century, with the largest increases in the East and West Southern Africa and Western Africa regions.

When all vegetation responses are included in S4, there is a reduction in median WSI for all regions, except for East Central Asia and the Sahara, when compared with S1 (Fig 8; left panel). The CO₂-induced stomatal response appears to be driving the largest reductions in WSI, indicated by CO₂: STOM and CO₂: STOM+VEG (Fig. 7; right panel). Reductions of 30-40% are projected for Madagascar, East Southern Africa and South-Eastern Africa regions, and 20-30% reductions in Western Africa,

Northeast South America, and South and East Asia. These regions are predominantly in tropical climates, aligning with the areas of increased water supply shown in Fig. 6b. However, CO₂: STOM+VEG also indicates increases in median WSI, potentially due to CO₂-induced vegetation growth in regions like North Central America, East Central Asia, and South and East Australia. Climate-induced vegetation changes (CLIM: VEG) appear to drive WSI reductions in almost all regions, perhaps due to decreased leaf area and vegetation coverage requiring less water in these regions. These reductions are considerable in some areas, with ~45% decreases in East and South Australia. When all dynamic vegetation responses are considered in CO₂: STOM & CLIM+CO₂: VEG, the majority of these most water scarce regions see a 20-40% reduction.

These results are reinforced by alternative WSI measures; both the number of severely water scarce months (Fig. S4a) and % area in severe water scarcity (Fig. S4b), indicate that incorporating dynamic plant processes leads to a reduction in both the temporal and spatial extent of water scarcity for most regions. These reductions are also primarily driven by the CO₂-induced reduction in stomatal aperture, particularly in the tropical regions such as East Asia and South-Eastern Africa.

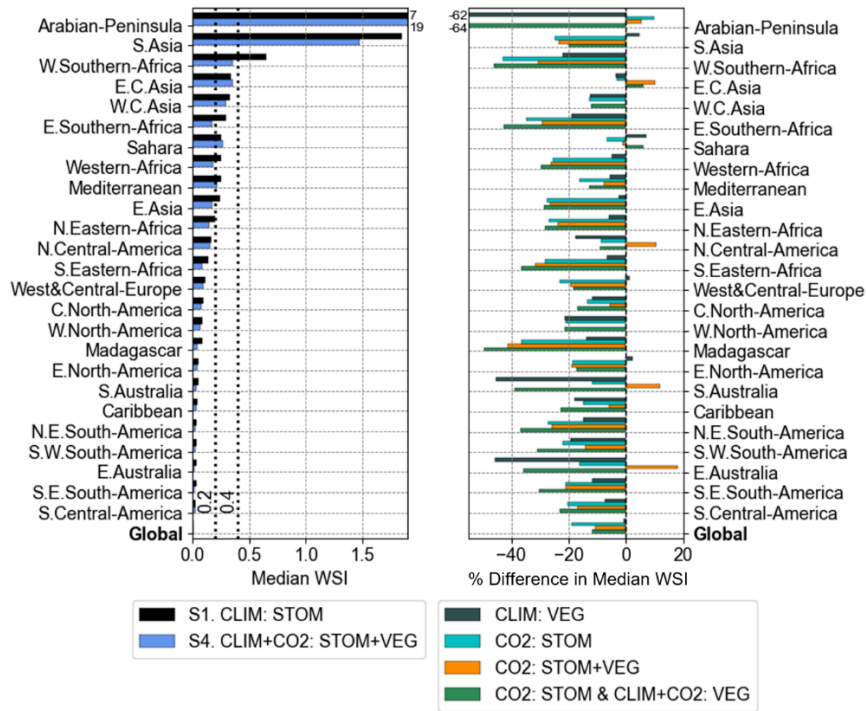


Figure 7: Median monthly WSI in simulations S1 and S4 (left) and % difference of median WSI when including the various isolated factors (right) by IPCC AR6 regions for the future period 2076-2095. The grey dashed lines (left) indicate the thresholds for mild water scarcity (WSI \geq 0.2) and severe water scarcity (WSI \geq 0.4). Only the 25 regions with the highest median WSI, according to the S1. CLIM: STOM simulation, are shown, sorted from the most water scarce region (top) to the least (bottom). The global median is also presented at the bottom. Out-of-range values for the Arabian-Peninsula are printed at the top.

When analysing median WSI by river basins for the future period (2076 – 2095; Fig. 8), the findings become clearer compared to the grid-cell analysis in Fig. 6. Similar to the bar plots in Fig. 7, the comparison of median WSI between scenarios S1 and S4 (Fig. 8a, b) suggests that dynamic plant processes results in limited overall changes. However, WSI category shifts are suggested for several basins, including in central, southern, and northern Africa, Southeast Asia, and eastern Australia.

Supporting our existing findings, the CO₂-induced stomatal response reduces WSI in many basins (Fig. 8c,d,f); median WSI at least 20% lower in numerous basins, including in Europe, central and southern Africa, and South and East Asia, and at least 40% lower in basins in part of Africa. When CO₂ effects on vegetation structure are also included in CO₂: STOM+VEG, median WSI increases by more than 10% in 18 basins (Table 2) including in the Middle East, Australia, Southern and Northwestern Africa, and the western USA (Fig. 8d), potentially due to CO₂-induced vegetation increases enhancing drying. However, the supply increases from stomatal responses due to enhanced CO₂ appear to dominate, resulting in WSI reductions by at least 10% in 122 basins (Table 2).

The effects of climate-induced vegetation structural changes is more varied with modest increases in WSI (<10%) in much of Europe and larger increases (10-30%) in central-northern Africa. However, reductions are more common, particularly around arid and semi-arid regions (Fig. 8e), also supported by Table 2, which suggests more increases than decreases in median WSI across all the thresholds.

Considering all factors combined (CO₂: STOM & CLIM+CO₂: VEG), decreases in WSI outweigh increases (Fig. 8f). Out of 291 basins, 139 show reductions of at least 10% (maximum 67%), affecting 80% of the global population, while only 11 basins see increases over 10% (maximum 59%), affecting just 0.2% of the population (Table 2). Most of the population are seeing small percentage changes compared with large ones, shown by the higher numbers in the lower thresholds (e.g., 5% and 10%) in Table 2. For example, when all processes are included in CO₂: STOM & CLIM+CO₂: VEG, median WSI will reduce by at least 5% for 88% of the population compared with reductions of at least 40% for only 2% of the population.

Figure S5 shows the number of months in severe water scarcity (WSI \geq 0.4), with the CO₂-induced stomatal response again driving small reductions of mainly 1 to 2 months in many basins, in similar regions to those seen in Fig. 8f, including southern South America, central and southern Africa southeast Asia and coastal Australia. The results are also consistent when dividing into seasons, which show overwhelming reductions in median WSI across all seasons in the future period (Fig. S6).

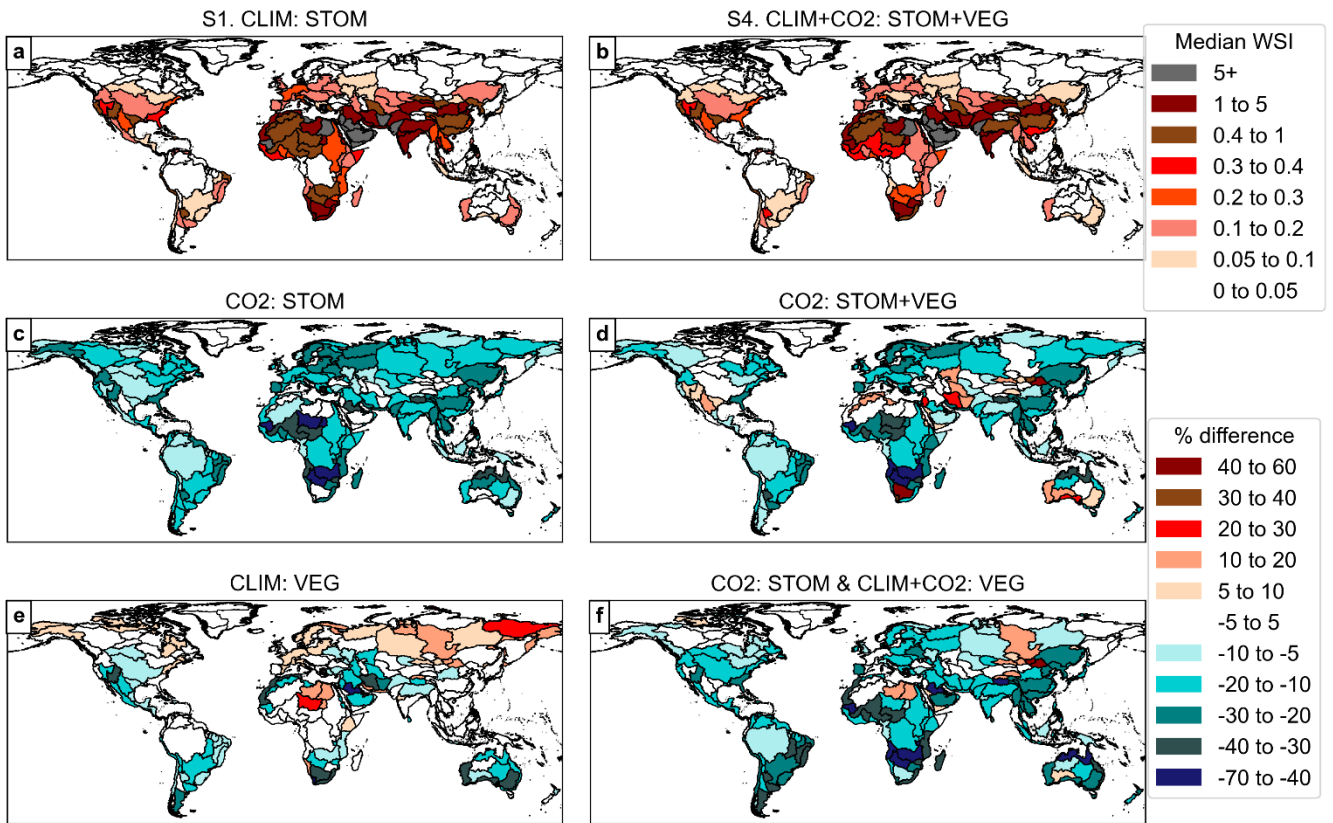


Figure 8: Median WSI in simulations S1 and S4 (top row) and the relative (%) difference in median WSI when including the various isolated factors by river basin for the future period 2076-2095.

Threshold (%)	Factor	Basin count above Threshold	Basin count below -Threshold	Percentage of population above Threshold	Percentage of population below -Threshold	
390	5	CO2: STOM	0	198	0.0	90.1
		CO2: STOM+VEG	26	169	4.4	83.5
		CLIM: VEG	51	76	7.3	33.4
		CO2: STOM & CLIM+CO2: VEG	17	176	1.1	87.8
395	10	CO2: STOM	0	156	0.0	81.4
		CO2: STOM+VEG	18	122	2.7	62.0
		CLIM: VEG	21	43	0.4	9.3
		CO2: STOM & CLIM+CO2: VEG	11	139	0.2	80.2
400	20	CO2: STOM	0	67	0.0	24.7
		CO2: STOM+VEG	7	56	1.0	21.4
		CLIM: VEG	5	15	0.1	2.6
		CO2: STOM & CLIM+CO2: VEG	4	68	0.0	26.4
410	40	CO2: STOM	0	9	0.0	1.6
		CO2: STOM+VEG	2	6	0.3	1.9
		CLIM: VEG	1	2	0.0	0.2
		CO2: STOM & CLIM+CO2: VEG	3	11	0.0	2.1

Table 2. Total number of river basins and the percentage of the total projected global population affected by changes in median WSI relative to specific percentage thresholds, driven by various isolated factors for the period 2076–2095.

405

The annual cycles of median WSI for the period 2076 to 2095 across several major river basins are illustrated in Fig. 9, along with the relative differences when the isolated factors are included. These basins were selected based on their population and water scarcity levels, ensuring a fair geographic distribution across all continents (excluding the poles).

410 All basins experience periods of water scarcity during parts of the year. Consistent with previous findings, the inclusion of the CO₂-induced stomatal response mitigates WSI in all basins throughout the year, and especially during water-scarce periods. In some basins, this effect reduces WSI by over 40% during certain times of the year. For instance, in the northwest Africa and Tigris-Euphrates basins (Fig. 9a,c), the WSI is projected to be at least 50% lower during the most water-scarce periods. The basin in southern Africa presents contrasting results to the other basins and to our existing results; when including the

415 CO₂-induced vegetation structural increases in CO2: STOM+VEG, median WSI is 50% higher, which is the case for much of the year. Interestingly, climate-induced vegetation structural changes drive 40-50% reduction in WSI over the year. These two processes appear to be balancing one another out, as the combined effect of all processes results in minimal net change in WSI.

Overall, including all plant responses to CO₂ and climate in S4, consistently mitigates WSI across the year in most basins, with the magnitude of these effects varying across the year. These findings suggest that plant responses to CO₂ have the most substantial impact during periods of water scarcity, highlighting their importance in future water scarcity projections.

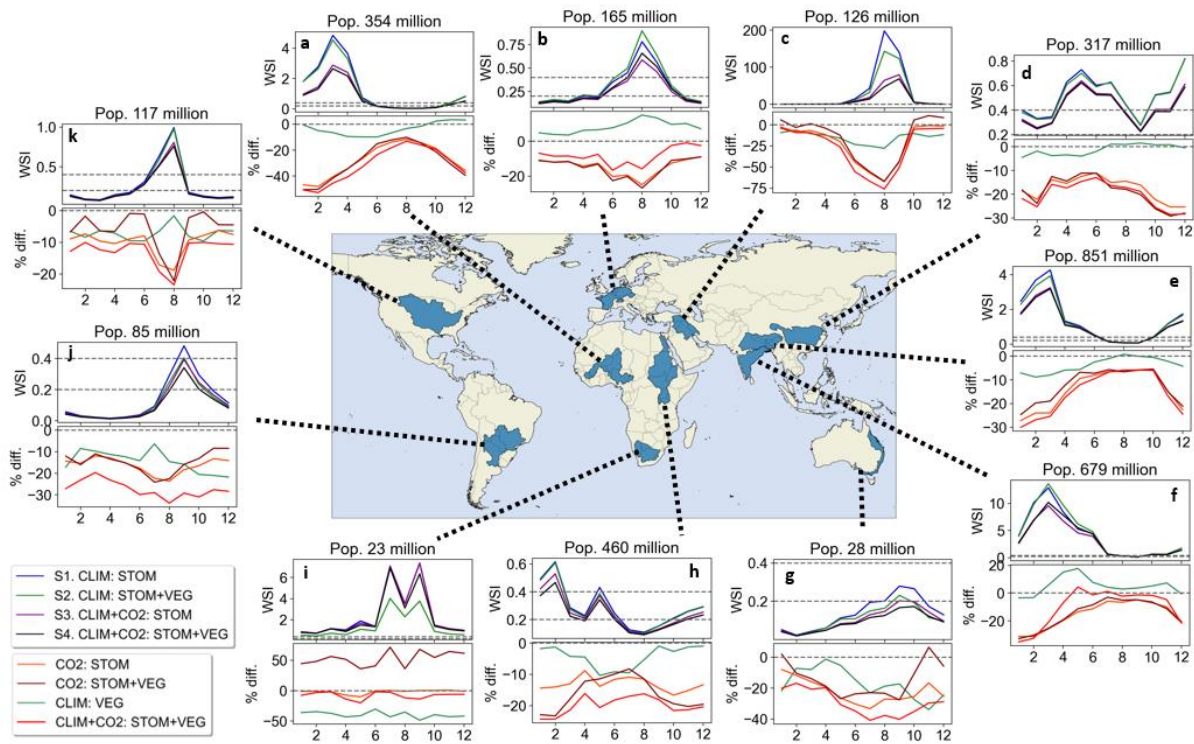


Figure 9: Annual cycles of median WSI, and the relative (%) difference in median WSI when including the various isolated factors for various river basins around the world for the future period 2076-2095. Total population of the basin is noted above each plot.

4 Discussion

Existing studies on the socioeconomic impacts of water scarcity are typically based on hydrology models that do not include plant physiological or structural responses to CO₂ or climate change (e.g., Dolan et al., 2021; Gosling and Arnell, 2016; Greve et al., 2018; Haddeland et al., 2014; Schewe et al., 2013). By replicating the common approach, i.e., driving a standalone impacts model with climate model output, this study investigates the influence of incorporating these plant responses in such analyses.

Numerous observational and modelling studies have demonstrated the impact of physiological forcing on the water cycle. In line with many of these studies (e.g., Betts et al., 2007; Cao et al., 2010; Gedney et al., 2006), our results suggest that, for the overall global mean, rising CO₂ decreases stomatal conductance and transpiration, leading to higher soil moisture and increased

runoff (Figs. 2 and 3). Projected total runoff increases of 10-12% by the end of the century (Fig. 2e) are analogous with the global mean values suggested in Betts et al. (2007) and Cao et al. (2010). The runoff increases from the stomatal response are most pronounced in the tropics (Fig. 3i), corroborating the findings of several studies (e.g., Davie et al., 2013; Fowler et al., 2019; Lemordant et al., 2018; Yang et al., 2019). Furthermore, also supported by these studies, our results suggest that global mean LAI increases with rising CO₂ (Fig. 2k,n), but, at the global scale, any reductions in runoff due to increased vegetation cover and LAI is outweighed by the increases in runoff due to the CO₂-induced stomatal response, since CO₂: STOM+VEG shows relative *increases* for global mean runoff and soil moisture (Fig. 2e-h). However, CO₂- and climate-induced vegetation increases are still projected to drive small decreases in runoff across large areas of the globe, especially semi-arid and arid regions, west USA, parts of mid-latitudes and Australia, supported by several studies (e.g., Piao et al., 2007; Ukkola et al., 2016). Even though these decreases appear negligible in number, water supply is already low in many of these regions and therefore a small decrease can greatly exacerbate water scarcity in these areas.

The increase in global runoff and thus water supply when all the plant responses are included in our simulations translates to reductions in global median WSI. Our results suggest that the wetting effect of the stomatal response to rising CO₂ has the dominating influence over the drying effect of increased vegetation structural response in most places, especially when aggregated by IPCC climate regions and river basins. Under RCP 6.0 and SSP2 “middle-of-the-road” scenarios, global median WSI increases until mid-century and then declines (Fig. 4c), although many places will still experience worsening water scarcity throughout the century (Fig. 6c). Water scarcity projections with and without dynamic plant processes (Figs. 6-8) do not present drastic differences, but the influence of plant responses, particularly the stomatal response to rising CO₂, still have a noticeable effect when the results are collated over larger areas. In most IPCC AR6 regions and river basins, median WSI is *lower* when all plant responses are included in CO₂: STOM & CLIM+CO₂: VEG (Figs. 7-8; Table 2). Although CO₂-induced stomatal closure substantially increases water supply by ~35% (Fig. 4d), it reduces WSI by only ~20% (Fig. 4e) by 2100. The smaller influence on WSI arises because the largest supply increases are due to the CO₂-induced stomatal response, which has most influence in non-water scarce regions with abundant water supply, such as tropical regions like the Amazon and Southeast Asia (Fig. 6f,g), which contribute less to WSI values.

Notable differences emerge when computing WSI at different spatial scales. At the grid-box level, plant responses often lead to increases in median WSI across many areas (Fig. 6), because local demand, particularly in urban areas, can often substantially exceed local supply, as runoff from surrounding grid-boxes is not accounted for. In contrast, at larger spatial scales, decreases in WSI are more common (Figs. 7 to 9), as aggregating supply and demand across broader areas generally lowers WSI. For river basins, total runoff is assumed to be accessible to all inhabitants within the basin, which smooths out local imbalances. While neither approach fully captures the complexity of water distribution and accessibility, this is not a critical limitation for this study, which is to assess the *relative* influence of vegetation responses on WSI rather than produce precise estimates.

Furthermore, our findings may overestimate WSI in places, as our proxy for water supply is total runoff estimated using JULES, which does not include some sources which can supplement water supply, such as groundwater extraction. Another consideration which could mean our WSI estimates are too high, is because water demand for irrigation is estimated by hydrology model 'H08', which, like many other hydrology models, does not account for physiological forcing. Additional atmospheric CO₂ generally makes crops more water-efficient, lowering water required for irrigation, and thus potentially alleviating water scarcity.

The HadGEM2-ES climate data driving JULES in this study has been bias corrected following the ISIMIP2b protocol, although some residual biases remain in the JULES version used (Mathison et al., 2023). For 1980–2006, their evaluation indicates negligible runoff biases for most river basins. However, slight runoff underestimations in China and the northern high latitudes translate to overestimations in WSI in our study. Conversely, slight runoff overestimations in eastern USA translate to underestimations in WSI in our study. To assess the influence of plant responses, we take the difference between two simulations that share similar biases, and thus this minimises overall biases. Non-linear biases may persist when comparing simulations with differing plant responses, but these are expected to be relatively small compared with other uncertainties inherent in such modelling studies.

JULES uses parameterisation schemes to represent hydrological and biophysical processes. For example, the stomatal conductance scheme (see Appendix B) simplifies a complex process which varies across species, ecosystems, and climates (Norby and Zak, 2011). Evaluating the accuracy of such parameterisation schemes on a global scale is a major challenge, primarily due to limited observational data. Experiments such as Free Air CO₂ Enrichment (FACE) have provided valuable insights into plant physiological responses to elevated CO₂, which are crucial for land surface model developments, but are currently at a small number of point locations. Model-data comparison studies suggest mixed performance at simulating CO₂ effects on water-use efficiency, with models performing well for some sites and species but poorly for others (De Kauwe et al., 2013; Walker et al., 2014). Although JULES has not yet been comprehensively assessed in these studies, its behaviour is expected to be broadly comparable to the models evaluated. Furthermore, some studies suggest that the magnitude of the CO₂-effect on river runoff records in JULES is reasonable within uncertainty bounds (Gedney et al., 2006, 2014).

Since only one land surface model was assessed in this study, further work could test additional models to examine the sensitivity of the results. We would anticipate broadly consistent outcomes across LSMs when testing the stomatal response, as many LSMs employ stomatal conductance parameterisation schemes derived from similar formulations. However, we would expect a wider spread of responses in LSMs when testing vegetation structural responses, given that different Dynamic Global Vegetation Models apply alternative approaches to dynamic vegetation compared with the TRIFFID scheme used in JULES (Sitch et al., 2008).

505 Finally, we recognise that, to mimic typical hydrology impact studies, JULES was run standalone driven by climate model
output, without feedbacks to the driving climate model. For example, disabling the stomatal response to rising CO₂ in JULES
typically increases transpiration (Fig. 2), which typically enhances atmospheric moisture affecting humidity, temperature, and
precipitation. Such feedbacks could amplify differences in water scarcity projections between simulations with and without
vegetation responses. Assessing the importance of these missing interactions could highlight the value of using hydrology
510 models coupled to the atmosphere for water scarcity assessments.

5 Conclusions

Our results suggest that including plant physiological and structural responses to rising CO₂ and associated climate change in
JULES partially moderates water scarcity in many regions throughout this century. Enhanced water-use efficiency driven by
CO₂-induced stomatal closure contributes to increased water availability, particularly the tropics. The supply increase translates
515 to decreases in WSI in many regions, although the largest increases in water supply occur in regions that already experience
abundant rainfall, such as the tropics, which are typically areas that do not suffer from water scarcity. Thus, when averaged
globally, the CO₂-induced stomatal response drives relatively smaller reductions in WSI than increases in water supply. Our
projections also indicate potential increases in WSI in certain semi-arid and arid regions, attributed to CO₂- and climate-induced
expansions in vegetation cover and leaf area, reducing water availability in already water-limited areas. When WSI is
520 calculated across IPCC climate regions and river basins, the incorporation of all dynamic plant responses partially moderates
projected WSI for most of the global population. Our findings highlight the need to incorporate vegetation dynamics, primarily
physiological forcing, into hydrology models to improve the robustness of water scarcity assessments.

We note that there are limitations inherent in modelling the complex interactions between the biosphere and hydrosphere under
525 changing climate conditions. The results presented here are based on assumptions and parameterisations within the JULES
land surface model. Further research is needed to refine these findings, particularly through the use of more advanced
representations of plant responses to elevated CO₂ and climate change, supported by observational data. Such efforts will
enhance the accuracy and reliability of future water scarcity projections, improving their utility for policymakers and water
resource managers.

530 Appendices

Appendix A

The four JULES simulations and calculations for the “isolated factors”

		Vegetation structure (includes coverage, LAI and canopy height)		Calculations for isolated factor(s):
		Dynamic vegetation off (fixed at preindustrial)	Dynamic vegetation on	
Plant physiology	277 ppm (fixed at preindustrial)	S1. CLIM: STOM	S2. CLIM: STOM+VEG	S2 - S1. CLIM: VEG
CO₂ levels in JULES	RCP 6.0	S3. CLIM+CO ₂ : STOM	S4. CLIM+CO ₂ : STOM+VEG	<i>Not used</i>
Calculations for isolated factor(s):		S3 - S1. CO₂: STOM	S4 - S2. CO₂: STOM+VEG	S4 - S1. CO₂: STOM & CLIM+CO₂: VEG

Table A1: The four JULES simulations driven by identical climate model output, and a combination of fixing plant CO₂ and structural vegetation responses.

535 Appendix B

Stomatal Conductance Scheme used in JULES

The version of JULES used in this study uses a coupled canopy conductance and photosynthesis model (Cox et al., 1998) where stomatal conductance to water vapour g_s (m s^{-1}) is based on:

$$g_s = -1.6A \frac{RT^*}{c_i - c_a} \quad (1)$$

540 where A is the net photosynthetic rate ($\text{mol CO}_2 \text{ m}^{-2} \text{ s}^{-1}$), R is the universal gas constant ($\text{J K}^{-1} \text{ mol}^{-1}$), T^* is the leaf surface temperature (K), c_i the internal CO₂ partial pressure (Pa), c_a the leaf surface CO₂ partial pressure (Pa) and factor of 1.6 accounting for molecular diffusivity differences between water and CO₂. Vapour deficit at the leaf surface (D , kg kg^{-1}) affects stomatal conductance through the gradient between c_a and c_i is based on the equation by Jacobs (1994):

$$\frac{c_i - \Gamma^*}{c_a - \Gamma^*} = f_0 \left(1 - \frac{D}{D_{crit}} \right) \quad (2)$$

545 where Γ^* is the photorespiration compensation point (Pa) and D_{crit} and f_0 are PFT-specific calibration parameters, which are directly related to the parameters from the Leuning (1995) model (for details see Cox et al., 1998). Potential non-stressed leaf level photosynthesis is calculated in JULES using the C3 and C4 photosynthesis models of Collatz et al. (1991) and Collatz et al. (1992) respectively.

550 The Jacobs formulation is a simplified version of the Leuning (1995) model, which in turn is based on the (Ball et al., 1987) model but depends on humidity deficit at the leaf surface instead of relative humidity.

Runoff processes in JULES

555 In this version of JULES, soil is divided into 4 layers, each with its own water content, which is determined by considering the inputs, such as precipitation, and outputs such as evapotranspiration and infiltration. The moisture content of each soil layer influences water movement, affecting how much percolates downward to deeper layers or moves horizontally as lateral flow. Additionally, in this version of JULES a TOPMODEL-type scheme is included, based on Clark and Gedney (2008) and Gedney and Cox (2003). This accounts for the influence of topography on soil moisture and runoff, enhancing JULES's ability to simulate the sub-grid spatial variability. Surface runoff is generated when precipitation exceeds the soil's infiltration capacity, when the soil becomes fully saturated, or when sub-grid scale inundation occurs. In TOPMODEL-based schemes, sub-surface runoff, or "baseflow", occurs with lateral flow below the water table, and its magnitude is influenced by soil moisture and soil type.

Code availability

565 Python has been used to conduct our analysis. Code is available on GitHub at <https://github.com/jessica-stacey/water-scarcity-plants-jules>.

Data availability

570 Output from JULES simulations can be made available upon request. Water demand data is available from the ISIMIP database (e.g., https://data.isimip.org/search/query/amanww/tree/ISIMIP2b/OutputData/water_global/h08/hadgem2-es/). Population data is also available from the ISIMIP database (<https://data.isimip.org/datasets/6eee7c61-4baa-4b1d-aa81-d854f217f07e/>).

Author contributions

JS: Conceptualisation, investigation, methodology, formal analysis, visualisation, writing draft
575 RAB: Conceptualisation, methodology, supervision, writing (review and editing)
AH: Supervision, methodology, validation, writing (review and editing)
LM: Supervision, writing (review and editing)
NG: Writing (review and editing)

580 Competing interests

The authors declare that they have no conflict of interest.

Acknowledgements

585 The authors would like to thank Dr Camilla Mathison and Dr Eleanor Burke for their dedicated effort in setting up the JULES ISIMIP2b suite and their guidance for getting it running. We are also thankful to Dr Chantelle Burton for her technical support to JS on the project. We would like to thank Dr Peter Greve for his support in providing early-stage data (ultimately not used

in this study), guidance on obtaining monthly water demand data and discussions on calculating the Water Scarcity Index. Finally, we would like to express our gratitude to the ISIMIP (Inter-Sectoral Impact Model Intercomparison Project) team for maintaining high-quality datasets and fostering collaboration across the scientific community which have greatly contributed to the advancement of climate impact research. Also, we acknowledge the use of OpenAI's ChatGPT to enhance the clarity and accessibility of text drafted by JS, and GitHub's Copilot to refine code developed by JS for data analysis and visualisation. All outputs were meticulously reviewed, verified, and edited by JS to ensure accuracy, relevance, and adherence to scientific standards.

595 **Financial support**

JS, RAB, AH and NG were supported by the Met Office Hadley Centre Climate Programme funded by the UK Department of Science, Innovation and Technology (DSIT). JS, RAB and NG were additionally supported by the AmazonFACE programme funded by the UK Foreign, Commonwealth and Development Office (FCDO) and JS and AH were further supported by the Climate Science for Service Partnership (CSSP) Brazil project funded by DSIT. LM acknowledges funding by UK Natural Environment Research Council project NE/W004895/1.

References

- Ball, J. T., Woodrow, I. E., and Berry, J. A.: A Model Predicting Stomatal Conductance and its Contribution to the Control of Photosynthesis under Different Environmental Conditions, in: *Progress in Photosynthesis Research: Volume 4 Proceedings of the VIIth International Congress on Photosynthesis Providence, Rhode Island, USA, August 10–15, 1986*, edited by: Biggins, J., Springer Netherlands, Dordrecht, 221–224, https://doi.org/10.1007/978-94-017-0519-6_48, 1987.
- Battipaglia, G., Saurer, M., Cherubini, P., Calfapietra, C., Mccarthy, H. R., Norby, R. J., and Francesca Cotrufo, M.: Elevated CO₂ increases tree-level intrinsic water use efficiency: Insights from carbon and oxygen isotope analyses in tree rings across three forest FACE sites, *New Phytologist*, 197, 544–554, <https://doi.org/10.1111/nph.12044>, 2013.
- Best, M. J., Pryor, M., Clark, D. B., Rooney, G. G., Essery, R. L. H., Ménard, C. B., Edwards, J. M., Hendry, M. A., Porson, A., Gedney, N., Mercado, L. M., Sitch, S., Blyth, E., Boucher, O., Cox, P. M., Grimmond, C. S. B., and Harding, R. J.: The Joint UK Land Environment Simulator (JULES), model description-Part 1: Energy and water fluxes, *Geosci. Model Dev*, 4, 677–699, <https://doi.org/10.5194/gmd-4-677-2011>, 2011.
- Betts, R. A., Cox, P. M., Lee, S. E., and Woodward, F. I.: Contrasting physiological and structural vegetation feedbacks in climate change simulations, *Nature*, 387, 796–799, <https://doi.org/10.1038/42924>, 1997.
- Betts, R. A., Boucher, O., Collins, M., Cox, P. M., Falloon, P. D., Gedney, N., Hemming, D. L., Huntingford, C., Jones, C. D., Sexton, D. M. H., and Webb, M. J.: Projected increase in continental runoff due to plant responses to increasing carbon dioxide, *Nature*, 448, 1037–1041, <https://doi.org/10.1038/nature06045>, 2007.

- Caretta, M. A., Mukherji, A., Arfanuzzaman, M., Betts, R. A., Gelfan, A., Hirabayashi, Y., Lissner, T. K., Liu, J., Gunn, E.
620 L., Morgan, R., Mwanga, S., Supratid, S., Pörtner, H.-O., Roberts, D. C., Tignor, M., Poloczanska, E. S., Mintenbeck, K.,
Alegria, A., Craig, M., Langsdorf, S., Löschke, S., Möller, V., Okem, A., and Rama, B.: 2022: Water., In: *Climate Change
2022: Impacts, Adaptation, and Vulnerability. Contribution of Working Group II to the Sixth Assessment Report of the
Intergovernmental Panel on Climate Change*, 551–712, <https://doi.org/10.1017/9781009325844.006.552>, 2022.
- Cao, L., Bala, G., Caldeira, K., Nemani, R., and Ban-Weiss, G.: Importance of carbon dioxide physiological forcing to future
625 climate change, *Proceedings of the National Academy of Sciences of the United States of America*, 107, 9513–9518,
<https://doi.org/10.1073/pnas.0913000107>, 2010.
- Clark, D. B. and Gedney, N.: Representing the effects of subgrid variability of soil moisture on runoff generation in a land
surface model, *Journal of Geophysical Research: Atmospheres*, 113, <https://doi.org/10.1029/2007JD008940>, 2008.
- Clark, D. B., Mercado, L. M., Sitch, S., Jones, C. D., Gedney, N., Best, M. J., Pryor, M., Rooney, G. G., Essery, R. L. H.,
630 Blyth, E., Boucher, O., Harding, R. J., Huntingford, C., and Cox, P. M.: The Joint UK Land Environment Simulator (JULES),
model description – Part 2: Carbon fluxes and vegetation dynamics, *Geoscientific Model Development*, 4, 701–722,
<https://doi.org/10.5194/gmd-4-701-2011>, 2011.
- Collatz, G. J., Ball, J. T., Grivet, C., and Berry, J. A.: Physiological and environmental regulation of stomatal conductance,
photosynthesis and transpiration: a model that includes a laminar boundary layer, *Agricultural and Forest Meteorology*, 54,
635 107–136, [https://doi.org/10.1016/0168-1923\(91\)90002-8](https://doi.org/10.1016/0168-1923(91)90002-8), 1991.
- Collatz, G., Ribas-Carbo, M., and Berry, J.: Coupled Photosynthesis-Stomatal Conductance Model for Leaves of C4 Plants,
Functional Plant Biology, 19, 519–538, <https://doi.org/10.1071/PP9920519>, 1992.
- Cowan, I. R.: Stomatal Behaviour and Environment, *Advances in Botanical Research*, 4, 117–228,
[https://doi.org/10.1016/S0065-2296\(08\)60370-5](https://doi.org/10.1016/S0065-2296(08)60370-5), 1978.
- 640 Cowling, S. A. and Field, C. B.: Environmental control of leaf area production: Implications for vegetation and land-surface
modeling, *Global Biogeochemical Cycles*, 17, 7-1-7–14, <https://doi.org/10.1029/2002GB001915>, 2003.
- Cox, P. M., Huntingford, C., and Harding, R. J.: A canopy conductance and photosynthesis model for use in a GCM land
surface scheme, 213, 79–94, 1998.
- Cox, P. M.: Description of the TRIFFID dynamic global vegetation model, *Theoretical and Applied Climatology*, 16, 2001.
- 645 Davie, J. C. S., Falloon, P. D., Kahana, R., Dankers, R., Betts, R., Portmann, F. T., Wisser, D., Clark, D. B., Ito, A., Masaki,
Y., Nishina, K., Fekete, B., Tessler, Z., Wada, Y., Liu, X., Tang, Q., Hagemann, S., Stacke, T., Pavlick, R., Schaphoff, S.,
Gosling, S. N., Franssen, W., and Arnell, N.: Comparing projections of future changes in runoff from hydrological and biome
models in ISI-MIP, *Earth System Dynamics*, 4, 359–374, <https://doi.org/10.5194/esd-4-359-2013>, 2013.
- De Kauwe, M. G., Medlyn, B. E., Zaehle, S., Walker, A. P., Dietze, M. C., Hickler, T., Jain, A. K., Luo, Y., Parton, W. J.,
650 Prentice, I. C., Smith, B., Thornton, P. E., Wang, S., Wang, Y.-P., Wårlind, D., Weng, E., Crous, K. Y., Ellsworth, D. S.,
Hanson, P. J., Seok Kim, H.-, Warren, J. M., Oren, R., and Norby, R. J.: Forest water use and water use efficiency at elevated :

- a model-data intercomparison at two contrasting temperate forest FACE sites, *Global Change Biology*, 19, 1759–1779, <https://doi.org/10.1111/gcb.12164>, 2013.
- Dolan, F., Lamontagne, J., Link, R., Hejazi, M., Reed, P., and Edmonds, J.: Evaluating the economic impact of water scarcity in a changing world, *Nature Communications*, 12, 1–10, <https://doi.org/10.1038/s41467-021-22194-0>, 2021.
- Falkenmark, M., Lundqvist, J., and Widstrand, C.: Macro-scale water scarcity requires micro-scale approaches. Aspects of vulnerability in semi-arid development., *Natural resources forum*, 13, 258–267, <https://doi.org/10.1111/j.1477-8947.1989.tb00348.x>, 1989.
- FAO, 2017: <https://www.fao.org/fao-stories/article/en/c/1185405/>.
- 660 Field, C. B., Jackson, R. B., and Mooney, H. A.: Stomatal responses to increased CO₂: implications from the plant to the global scale, *Plant, Cell & Environment*, 18, 1214–1225, <https://doi.org/10.1111/j.1365-3040.1995.tb00630.x>, 1995.
- Fisher, R. A. and Koven, C. D.: Perspectives on the Future of Land Surface Models and the Challenges of Representing Complex Terrestrial Systems, *Journal of Advances in Modeling Earth Systems*, 12, e2018MS001453, <https://doi.org/10.1029/2018MS001453>, 2020.
- 665 Fowler, M. D., Kooperman, G. J., Randerson, J. T., and Pritchard, M. S.: The effect of plant physiological responses to rising CO₂ on global streamflow, *Nature Climate Change*, 9, 873–879, <https://doi.org/10.1038/s41558-019-0602-x>, 2019.
- Gedney, N. and Cox, P. M.: The Sensitivity of Global Climate Model Simulations to the Representation of Soil Moisture Heterogeneity, 2003.
- Gedney, N., Cox, P. M., Betts, R. A., Boucher, O., Huntingford, C., and Stott, P. A.: Detection of a direct carbon dioxide effect in continental river runoff records, *Nature*, 439, 835–838, <https://doi.org/10.1038/nature04504>, 2006.
- 670 Gedney, N., Huntingford, C., Weedon, G. P., Bellouin, N., Boucher, O., and Cox, P. M.: Detection of solar dimming and brightening effects on Northern Hemisphere river flow, *Nature Geosci*, 7, 796–800, <https://doi.org/10.1038/ngeo2263>, 2014.
- Gosling, S. N. and Arnell, N. W.: A global assessment of the impact of climate change on water scarcity, *Climatic Change*, 134, 371–385, <https://doi.org/10.1007/s10584-013-0853-x>, 2016.
- 675 Gosling, S. N., Müller Schmied, H., Burek, P., Chang, J., Ciais, P., Döll, P., Eisner, S., Fink, G., Flörke, M., Franssen, W., Grillakis, M., Hagemann, S., Hanasaki, N., Koutroulis, A., Leng, G., Liu, X., Masaki, Y., Mathison, C., Mishra, V., Ostberg, S., Portmann, F., Qi, W., Sahu, R.-K., Satoh, Y., Schewe, J., Seneviratne, S., Shah, H. L., Stacke, T., Tao, F., Telteu, C., Thiery, W., Trautmann, T., Tsanis, I., Wanders, N., Zhai, R., Büchner, M., Schewe, J., and Zhao, F.: ISIMIP2b Simulation Data from the Global Water Sector, <https://doi.org/10.48364/ISIMIP.626689>, 2023.
- 680 Greve, P., Kahil, T., Mochizuki, J., Schinko, T., Satoh, Y., Burek, P., Fischer, G., Tramberend, S., Burtscher, R., Langan, S., and Wada, Y.: Global assessment of water challenges under uncertainty in water scarcity projections, *Nature Sustainability*, 1, 486–494, <https://doi.org/10.1038/s41893-018-0134-9>, 2018.
- Haddeland, I., Heinke, J., Biemans, H., Eisner, S., Flörke, M., Hanasaki, N., Konzmann, M., Ludwig, F., Masaki, Y., Schewe, J., Stacke, T., Tessler, Z. D., Wada, Y., and Wisser, D.: Global water resources affected by human interventions and climate

- 685 change, *Proceedings of the National Academy of Sciences of the United States of America*, 111, 3251–3256, <https://doi.org/10.1073/pnas.1222475110>, 2014.
- Hanasaki, N., Kanae, S., Oki, T., Masuda, K., Motoya, K., Shirakawa, N., Shen, Y., and Tanaka, K.: An integrated model for the assessment of global water resources - Part 1: Model description and input meteorological forcing, *Hydrology and Earth System Sciences*, 12, 1007–1025, <https://doi.org/10.5194/hess-12-1007-2008>, 2008a.
- 690 Hanasaki, N., Kanae, S., Oki, T., Masuda, K., Motoya, K., Shirakawa, N., Shen, Y., and Tanaka, K.: An integrated model for the assessment of global water resources – Part 2: Applications and assessments, *Hydrology and Earth System Sciences*, 12, 1027–1037, <https://doi.org/10.5194/hess-12-1027-2008>, 2008b.
- Hanasaki, N., Yoshikawa, S., Pokhrel, Y., and Kanae, S.: A global hydrological simulation to specify the sources of water used by humans, *Hydrology and Earth System Sciences*, 22, 789–817, <https://doi.org/10.5194/hess-22-789-2018>, 2018.
- 695 Harper, A. B., Cox, P. M., Friedlingstein, P., Wiltshire, A. J., Jones, C. D., Sitch, S., Mercado, L. M., Groenendijk, M., Robertson, E., Kattge, J., Bönisch, G., Atkin, O. K., Bahn, M., Cornelissen, J., Niinemets, Ü., Onipchenko, V., Peñuelas, J., Poorter, L., Reich, P. B., Soudzilovskaia, N. A., and Bodegom, P. van: Improved representation of plant functional types and physiology in the Joint UK Land Environment Simulator (JULES v4.2) using plant trait information, *Geoscientific Model Development*, 9, 2415–2440, <https://doi.org/10.5194/gmd-9-2415-2016>, 2016.
- 700 Iturbide, M., Gutiérrez, J. M., Alves, L. M., Bedia, J., Cerezo-Mota, R., Gimeno, E., Cofiño, A. S., Di Luca, A., Faria, S. H., Gorodetskaya, I. V., Hauser, M., Herrera, S., Hennessy, K., Hewitt, H. T., Jones, R. G., Krakovska, S., Manzanar, R., Martínez-Castro, D., Narisma, G. T., Nurhati, I. S., Pinto, I., Seneviratne, S. I., van den Hurk, B., and Vera, C. S.: An update of IPCC climate reference regions for subcontinental analysis of climate model data: definition and aggregated datasets, *Earth System Science Data*, 12, 2959–2970, <https://doi.org/10.5194/essd-12-2959-2020>, 2020.
- 705 Jacobs, C. M. J.: *Direct Impact of Atmospheric CO₂ Enrichment on Regional Transpiration*, Wageningen Agricultural University, Ph.D. Thesis, 1994.
- Jones, C. D., Hughes, J. K., Bellouin, N., Hardiman, S. C., Jones, G. S., Knight, J., Liddicoat, S., O’Connor, F. M., Andres, R. J., Bell, C., Boo, K. O., Bozzo, A., Butchart, N., Cadule, P., Corbin, K. D., Doutriaux-Boucher, M., Friedlingstein, P., Gornall, J., Gray, L., Halloran, P. R., Hurtt, G., Ingram, W. J., Lamarque, J. F., Law, R. M., Meinshausen, M., Osprey, S., Palin, E. J.,
- 710 Parsons Chini, L., Raddatz, T., Sanderson, M. G., Sellar, A. A., Schurer, A., Valdes, P., Wood, N., Woodward, S., Yoshioka, M., and Zerroukat, M.: The HadGEM2-ES implementation of CMIP5 centennial simulations, *Geoscientific Model Development*, 4, 543–570, <https://doi.org/10.5194/gmd-4-543-2011>, 2011.
- Kooperman, G. J., Fowler, M. D., Hoffman, F. M., Koven, C. D., Lindsay, K., Pritchard, M. S., Swann, A. L. S., and Randerson, J. T.: Plant Physiological Responses to Rising CO₂ Modify Simulated Daily Runoff Intensity With Implications for Global-
- 715 Scale Flood Risk Assessment, *Geophysical Research Letters*, 45, 12,457-12,466, <https://doi.org/10.1029/2018GL079901>, 2018.
- Lange, S.: Trend-preserving bias adjustment and statistical downscaling with ISIMIP3BASD (v1.0), *Geoscientific Model Development*, 12, 3055–3070, <https://doi.org/10.5194/gmd-12-3055-2019>, 2019.

- Lehner, B. and Grill, G.: Global river hydrography and network routing: baseline data and new approaches to study the world's large river systems, *Hydrological Processes*, 27, 2171–2186, <https://doi.org/10.1002/hyp.9740>, 2013.
- Lemordant, L., Gentine, P., Swann, A. S., Cook, B. I., and Scheff, J.: Critical impact of vegetation physiology on the continental hydrologic cycle in response to increasing CO₂, *Proceedings of the National Academy of Sciences of the United States of America*, 115, 4093–4098, <https://doi.org/10.1073/pnas.1720712115>, 2018.
- Leuning, R.: A critical appraisal of a combined stomatal-photosynthesis model for C₃ plants, *Plant, Cell & Environment*, 18, 339–355, <https://doi.org/10.1111/j.1365-3040.1995.tb00370.x>, 1995.
- Mankin, J. S., Seager, R., Smerdon, J. E., Cook, B. I., and Williams, A. P.: Mid-latitude freshwater availability reduced by projected vegetation responses to climate change, *Nature Geoscience*, 12, 983–988, <https://doi.org/10.1038/s41561-019-0480-x>, 2019.
- Mathison, C., Burke, E., Hartley, A. J., Kelley, D. I., Burton, C., Robertson, E., Gedney, N., Williams, K., Wiltshire, A., Ellis, R. J., Sellar, A. A., and Jones, C. D.: Description and evaluation of the JULES-ES set-up for ISIMIP2b, *Geoscientific Model Development*, 16, 4249–4264, <https://doi.org/10.5194/gmd-16-4249-2023>, 2023.
- Norby, R. J. and Zak, D. R.: Ecological lessons from free air carbon enhancement (FACE) experiments, *Annual Review of Ecology, Evolution, and Systematics*, 42, <https://doi.org/10.1146/annurev-ecolsys-102209-144647>, 2011.
- Parmesan, C., Morecroft, M. D., Trisurat, Y., Adrian, R., Anshari, G. Z., Arneth, A., Gao, Q., Gonzalez, P., Harris, R., Price, J., Stevens, N., and Talukdar, G. H.: Terrestrial and freshwater ecosystems and their services, in: *Climate Change 2022: Impacts, Adaptation and Vulnerability, Contribution of Working Group II to the Sixth Assessment Report of the Intergovernmental Panel on Climate Change*, edited by: Pörtner, H.-O., Roberts, D. C., Tignor, M., Poloczanska, E. S., Mintenbeck, K., Alegría, A., Craig, M., Langsdorf, S., Lösschke, S., Möller, V., Okem, A., and Rama, B., Cambridge University Press, Cambridge, UK and New York, NY, USA, 197–377, <https://doi.org/10.1017/9781009325844.004>, 2022.
- Piao, S., Friedlingstein, P., Ciais, P., De Noblet-Ducoudré, N., Labat, D., and Zaehle, S.: Changes in climate and land use have a larger direct impact than rising CO₂ on global river runoff trends, *Proceedings of the National Academy of Sciences of the United States of America*, 104, 15242–15247, <https://doi.org/10.1073/pnas.0707213104>, 2007.
- Piontek, F. and Geiger, T.: ISIMIP2b secondary population input data (1.0), <https://doi.org/10.48364/ISIMIP.432399>, 2017.
- Raskin, P. and Gleick, P. H.: *Water Futures: Assessment of Long-range Patterns and Problems*, Stockholm Environment Institute, Stockholm, 1997.
- Riahi, K., van Vuuren, D. P., Kriegler, E., Edmonds, J., O'Neill, B. C., Fujimori, S., Bauer, N., Calvin, K., Dellink, R., Fricko, O., Lutz, W., Popp, A., Cuaresma, J. C., KC, S., Leimbach, M., Jiang, L., Kram, T., Rao, S., Emmerling, J., Ebi, K., Hasegawa, T., Havlik, P., Humpenöder, F., Da Silva, L. A., Smith, S., Stehfest, E., Bosetti, V., Eom, J., Gernaat, D., Masui, T., Rogelj, J., Strefler, J., Drouet, L., Krey, V., Luderer, G., Harmsen, M., Takahashi, K., Baumstark, L., Doelman, J. C., Kainuma, M., Klimont, Z., Marangoni, G., Lotze-Campen, H., Obersteiner, M., Tabeau, A., and Tavoni, M.: The Shared Socioeconomic Pathways and their energy, land use, and greenhouse gas emissions implications: An overview, *Global Environmental Change*, 42, 153–168, <https://doi.org/10.1016/j.gloenvcha.2016.05.009>, 2017.

- Ripple, W. J., Wolf, C., Newsome, T. M., Galetti, M., Alamgir, M., Crist, E., Mahmoud, M. I., Laurance, W. F., and 15,364 scientist signatories from 184 countries: World Scientists' Warning to Humanity: A Second Notice, *BioScience*, 67, 1026–1028, <https://doi.org/10.1093/biosci/bix125>, 2017.
- Schewe, J., Heinke, J., Gerten, D., Haddeland, I., Arnell, N. W., Clark, D. B., Dankers, R., Eisner, S., Fekete, B. M., Colón-González, F. J., Gosling, S. N., Kim, H., Liu, X., Masaki, Y., Portmann, F. T., Satoh, Y., Stacke, T., Tang, Q., Wada, Y., Wisser, D., Albrecht, T., Frieler, K., Piontek, F., Warszawski, L., and Kabat, P.: Multimodel assessment of water scarcity under climate change, *Proceedings of the National Academy of Sciences of the United States of America*, 111, 3245–3250, <https://doi.org/10.1073/pnas.1222460110>, 2013.
- Schneider, U., Finger, P., Meyer-Christoffer, A., Rustemeier, E., Ziese, M., and Becker, A.: Evaluating the hydrological cycle over land using the newly-corrected precipitation climatology from the Global Precipitation Climatology Centre (GPCP), *Atmosphere*, 8, <https://doi.org/10.3390/atmos8030052>, 2017.
- Sellar, A. A., Jones, C. G., Mulcahy, J. P., Tang, Y., Yool, A., Wiltshire, A., O'Connor, F. M., Stringer, M., Hill, R., Palmieri, J., Woodward, S., de Mora, L., Kuhlbrodt, T., Rumbold, S. T., Kelley, D. I., Ellis, R., Johnson, C. E., Walton, J., Abraham, N. L., Andrews, M. B., Andrews, T., Archibald, A. T., Berthou, S., Burke, E., Blockley, E., Carslaw, K., Dalvi, M., Edwards, J., Folberth, G. A., Gedney, N., Griffiths, P. T., Harper, A. B., Hendry, M. A., Hewitt, A. J., Johnson, B., Jones, A., Jones, C. D., Keeble, J., Liddicoat, S., Morgenstern, O., Parker, R. J., Predoi, V., Robertson, E., Siahahaan, A., Smith, R. S., Swaminathan, R., Woodhouse, M. T., Zeng, G., and Zerroukat, M.: UKESM1: Description and Evaluation of the U.K. Earth System Model, *Journal of Advances in Modeling Earth Systems*, 11, 4513–4558, <https://doi.org/10.1029/2019MS001739>, 2019.
- Seneviratne, S. I., Zhang, X., Adnan, M., Badi, W., Dereczynski, C., Luca, A. D., Ghosh, S., Iskandar, I., Kossin, J., Lewis, S., Otto, F., Pinto, I., Satoh, M., Vicente-Serrano, S. M., Wehner, M., Zhou, B. and Allan, R.: Weather and climate extreme events in a changing climate, *Climate Change 2021: The Physical Science Basis: Working Group I contribution to the Sixth Assessment Report of the Intergovernmental Panel on Climate Change*. Cambridge University Press, 1513–1766, <https://doi.org/10.1017/9781009157896.013>, 2021.
- Sitch, S., Huntingford, C., Gedney, N., Levy, P. E., Lomas, M., Piao, S. L., Betts, R., Ciais, P., Cox, P., Friedlingstein, P., Jones, C. D., Prentice, I. C., and Woodward, F. I.: Evaluation of the terrestrial carbon cycle, future plant geography and climate-carbon cycle feedbacks using five Dynamic Global Vegetation Models (DGVMs), *Global Change Biology*, 14, 2015–2039, <https://doi.org/10.1111/j.1365-2486.2008.01626.x>, 2008.
- Sitch, S., O'Sullivan, M., Robertson, E., Friedlingstein, P., Albergel, C., Anthoni, P., Arneeth, A., Arora, V. K., Bastos, A., Bastrikov, V., Bellouin, N., Canadell, J. G., Chini, L., Ciais, P., Falk, S., Harris, I., Hurtt, G., Ito, A., Jain, A. K., Jones, M. W., Joos, F., Kato, E., Kennedy, D., Klein Goldewijk, K., Kluzek, E., Knauer, J., Lawrence, P. J., Lombardozzi, D., Melton, J. R., Nabel, J. E. M. S., Pan, N., Peylin, P., Pongratz, J., Poulter, B., Rosan, T. M., Sun, Q., Tian, H., Walker, A. P., Weber, U., Yuan, W., Yue, X., and Zaehle, S.: Trends and Drivers of Terrestrial Sources and Sinks of Carbon Dioxide: An Overview of the TRENDY Project, *Global Biogeochemical Cycles*, 38, e2024GB008102, <https://doi.org/10.1029/2024GB008102>, 2024.

- Swann, A. L. S., Hoffman, F. M., Koven, C. D., and Randerson, J. T.: Plant responses to increasing CO₂ reduce estimates of climate impacts on drought severity, *Proceedings of the National Academy of Sciences of the United States of America*, 113, 10019–10024, <https://doi.org/10.1073/pnas.1604581113>, 2016.
- Ukkola, A. M., Prentice, I. C., Keenan, T. F., Van Dijk, A. I. J. M., Viney, N. R., Myneni, R. B., and Bi, J.: Reduced streamflow in water-stressed climates consistent with CO₂ effects on vegetation, <https://doi.org/10.1038/NCLIMATE2831>, 2016.
- Walker, A. P., Hanson, P. J., De Kauwe, M. G., Medlyn, B. E., Zaehle, S., Asao, S., Dietze, M., Hickler, T., Huntingford, C., Iversen, C. M., Jain, A., Lomas, M., Luo, Y., McCarthy, H., Parton, W. J., Prentice, I. C., Thornton, P. E., Wang, S., Wang, Y.-P., Warlind, D., Weng, E., Warren, J. M., Woodward, F. I., Oren, R., and Norby, R. J.: Comprehensive ecosystem model-data synthesis using multiple data sets at two temperate forest free-air CO₂ enrichment experiments: Model performance at ambient CO₂ concentration, *Journal of Geophysical Research: Biogeosciences*, 119, 937–964, <https://doi.org/10.1002/2013JG002553>, 2014.
- Wang, T. and Sun, F.: Socioeconomic exposure to drought under climate warming and globalization: The importance of vegetation-CO₂ feedback, *International Journal of Climatology*, n/a, <https://doi.org/10.1002/joc.8174>, 2023.
- Wei, H., Zhang, Y., Huang, Q., Chiew, F. H. S., Luan, J., Xia, J., and Liu, C.: Direct vegetation response to recent CO₂ rise shows limited effect on global streamflow, *Nat Commun*, 15, 9423, <https://doi.org/10.1038/s41467-024-53879-x>, 2024.
- Wei, Z., Yoshimura, K., Wang, L., Miralles, D. G., Jasechko, S., and Lee, X.: Revisiting the contribution of transpiration to global terrestrial evapotranspiration, *Geophysical Research Letters*, 44, 2792–2801, <https://doi.org/10.1002/2016GL072235>, 2017.
- Wigley, T. M. L. and Jones, P. D.: Influences of precipitation changes and direct CO₂ effects on streamflow, *Nature*, 314, 149–152, <https://doi.org/10.1038/314149a0>, 1985.
- Wiltshire, A., Gornall, J., Booth, B., Dennis, E., Falloon, P., Kay, G., McNeall, D., McSweeney, C., and Betts, R.: The importance of population, climate change and CO₂ plant physiological forcing in determining future global water stress, *Global Environmental Change*, 23, 1083–1097, <https://doi.org/10.1016/j.gloenvcha.2013.06.005>, 2013a.
- Wiltshire, A. J., Kay, G., Gornall, J. L., and Betts, R. A.: The impact of climate, CO₂ and population on regional food and water resources in the 2050s, *Sustainability (Switzerland)*, 5, 2129–2151, <https://doi.org/10.3390/su5052129>, 2013b.
- Xu, H., Wang, X., and Yang, T.: Trend shifts in satellite-derived vegetation growth in Central Eurasia, 1982–2013, *Science of The Total Environment*, 579, 1658–1674, <https://doi.org/10.1016/j.scitotenv.2016.11.182>, 2017.
- Yang, H., Huntingford, C., Wiltshire, A., Sitch, S., and Mercado, L.: Compensatory climate effects link trends in global runoff to rising atmospheric CO₂ concentration, *Environmental Research Letters*, 14, 124075, <https://doi.org/10.1088/1748-9326/ab5c6f>, 2019.
- Yu, T., Sun, R., Xiao, Z., Zhang, Q., Liu, G., Cui, T., and Wang, J.: Estimation of Global Vegetation Productivity from Global LAnd Surface Satellite Data, *Remote Sensing*, 10, 327, <https://doi.org/10.3390/rs10020327>, 2018.
- Zhu, Z., Piao, S., Myneni, R. B., Huang, M., Zeng, Z., Canadell, J. G., Ciais, P., Sitch, S., Friedlingstein, P., Arneeth, A., Cao, C., Cheng, L., Kato, E., Koven, C., Li, Y., Lian, X., Liu, Y., Liu, R., Mao, J., Pan, Y., Peng, S., Peuelas, J., Poulter, B., Pugh,

820 T. A. M., Stocker, B. D., Viovy, N., Wang, X., Wang, Y., Xiao, Z., Yang, H., Zaehle, S., and Zeng, N.: Greening of the Earth and its drivers, *Nature Climate Change*, 6, 791–795, <https://doi.org/10.1038/nclimate3004>, 2016.